JOURNAL OF BACTERIOLOGY, July 2007, p. 4984–4993 Vol. 189, No. 14
0021-9193/07/$08.00+0 doi:10.1128/JB.00530-07

Transcription Activation by the DNA-Binding Domain of the AraC Family Protein RhaS in the Absence of Its Effector-Binding Domain▽

Jason R. Wickstrum,[1]† Jeff M. Skredenske,[1] Ana Kolin,[1]‡ Ding J. Jin,[2] Jianwen Fang,[3] and Susan M. Egan[1]*

Department of Molecular Biosciences, University of Kansas, Lawrence, Kansas 66045[1]; Transcription Control Section, Gene Regulation and Chromosome Biology Laboratory, Center for Cancer Research, National Cancer Institute at Frederick, NIH, Bldg. 469, P.O. Box B, Frederick, Maryland 21702[2]; and Bioinformatics Core Facility, University of Kansas, Lawrence, Kansas 66045[3]

Received 6 April 2007/Accepted 9 May 2007

The *Escherichia coli* L-rhamnose-responsive transcription activators RhaS and RhaR both consist of two domains, a C-terminal DNA-binding domain and an N-terminal dimerization domain. Both function as dimers and only activate transcription in the presence of L-rhamnose. Here, we examined the ability of the DNA-binding domains of RhaS (RhaS-CTD) and RhaR (RhaR-CTD) to bind to DNA and activate transcription. RhaS-CTD and RhaR-CTD were both shown by DNase I footprinting to be capable of binding specifically to the appropriate DNA sites. In vivo as well as in vitro transcription assays showed that RhaS-CTD could activate transcription to high levels, whereas RhaR-CTD was capable of only very low levels of transcription activation. As expected, RhaS-CTD did not require the presence of L-rhamnose to activate transcription. The upstream half-site at *rhaBAD* and the downstream half-site at *rhaT* were found to be the strongest of the known RhaS half-sites, and a new putative RhaS half-site with comparable strength to known sites was identified. Given that cyclic AMP receptor protein (CRP), the second activator required for full *rhaBAD* expression, cannot activate *rhaBAD* expression in a Δ*rhaS* strain, it was of interest to test whether CRP could activate transcription in combination with RhaS-CTD. We found that RhaS-CTD allowed significant activation by CRP, both in vivo and in vitro, although full-length RhaS allowed somewhat greater CRP activation. We conclude that RhaS-CTD contains all of the determinants necessary for transcription activation by RhaS.

The RhaS protein functions to activate transcription of two of the operons in the *Escherichia coli* L-rhamnose regulon in response to the availability of L-rhamnose (11, 40). The two operons *rhaBAD* and *rhaT* encode the L-rhamnose catabolic enzymes (L-rhamnulokinase, L-rhamnose isomerase, and L-rhamnulose-1-phosphate aldolase) (2, 25) and an L-rhamnose-proton symporter that is responsible for transporting L-rhamnose into the cell (35), respectively. RhaS is encoded in an operon that also encodes a second L-rhamnose-responsive transcription activator, RhaR (37). RhaR activates transcription of the operon that encodes the two activator proteins, *rhaSR* (37, 38). All three operons in the L-rhamnose regulon also require a second activator protein, cyclic AMP (cAMP) receptor protein (CRP), for full transcription activation (11, 16, 40).

RhaS and RhaR are both members of the AraC/XylS family of transcription activators. This very large family of transcription activators is defined by sequence similarity in a 100-amino-acid region (10, 13). In all studied AraC/XylS family members, this 100-amino-acid region functions as a DNA-binding domain and is referred to here as the AraC/XylS family domain. Most family members contain one or more domains in addition to the AraC/XylS family domain, but a few family members consist only of this single domain, such as MarA and SoxS (13). AraC and XylS, the namesakes of the family, are examples of two-domain family members in which the nonfamily domain functions in both effector binding and dimerization (7, 19, 33).

Detailed molecular structures have been determined for the DNA-binding domains of two AraC/XylS family members, MarA and Rob (20, 28). MarA and Rob share particularly high sequence similarity, 51%, and the structures of their DNA-binding domains (the only domain of MarA) are nearly identical (with a root mean square deviation of 0.9 Å) (20). The DNA-binding domain of AraC/XylS family members contains two helix-turn-helix (HTH) DNA-binding motifs that contact consecutive major grooves of the DNA (20, 28). As a consequence, the binding site for each monomer (referred to as a half-site for dimers) is at least 17 bp long (13). In addition to DNA binding, the AraC/XylS family domain of a number of family members has been shown to be involved in transcription activation, making contacts with the C-terminal domain of the alpha subunit (α-CTD) of RNA polymerase (RNAP), the σ^{70} subunit of RNAP, or both (reviewed in reference 21).

Although membership in the AraC family is defined by sequence similarity within a single domain, RhaS and RhaR share amino acid sequence identity with each other, as well as with AraC, over their entire lengths. All three proteins are therefore predicted to have similar three-dimensional structures for both of their domains. The RhaS and RhaR N-

* Corresponding author. Mailing address: Department of Molecular Biosciences, 1200 Sunnyside Ave., University of Kansas, Lawrence, KS 66045. Phone: (785) 864-4294. Fax: (785) 864-5294. E-mail: sme@ku.edu.

† Present address: Department of Microbiology, Molecular Genetics and Immunology, University of Kansas Medical Center, Kansas City, KS 66160.

‡ Present address: Department of Microbiology and Immunology, 4301 Jones Bridge Road, Uniformed Services University of the Health Sciences, Bethesda, MD 20814.

▽ Published ahead of print on 18 May 2007.

terminal domains (NTDs) function in both ligand binding and dimerization (A. Kolin and S. Egan, unpublished results), while the CTDs are responsible for both DNA binding and direct contact with RNAP to activate transcription (4, 5, 42). We have previously identified several amino acid-base pair contacts that are involved in DNA binding by RhaS at *rhaBAD* (4). We have also identified two residues in RhaS and one in RhaR that are required to contact the σ^{70} subunit of RNAP to activate transcription and further have identified the residues in σ^{70} that each of these activator residues contacts (5, 42). Interestingly, the RhaS and RhaR residues involved in these contacts with σ^{70} are all located in one of the HTH motifs of the proteins.

Among AraC/XylS family proteins that consist of more than one domain, it is interesting that there have been a variety of findings regarding whether the DNA-binding domain alone is sufficient to activate transcription (7, 18, 19, 24, 26, 36). One example is the *Pseudomonas putida* activator XylS (XylS-ΔN209). When overexpressed to sufficiently high levels, XylS-ΔN209 can activate transcription of the TOL plasmid *Pm* promoter to the same high level as full-length XylS (19). Interestingly, at this high level of expression, full-length XylS becomes independent of its effector, activating to the same high levels in the absence and the presence of ligand. Another example is the DNA-binding domain of AraC. This domain alone could activate transcription of *araBAD* up to 15% as well as full-length AraC when alone or to the same level as full-length AraC when fused to an unrelated dimerization domain (7, 36). In contrast, the DNA-binding domain of the MelR protein (MelR173) is unable to activate transcription either at the wild-type target promoter (p*melAB*) or at promoters where the promoter-proximal MelR half-site is improved (18; S. Busby, personal communication).

In the present study, we tested the C-terminal AraC/XylS family domains of RhaS and RhaR for their ability to bind DNA and activate transcription in the absence of their NTDs. We found that, while RhaS-CTD was able to activate transcription to high levels, RhaR-CTD could only activate to very low levels. DNase I footprinting indicated that both purified RhaS-CTD and RhaR-CTD were able to bind to DNA at their respective binding sites. Comparison of all of the RhaS half-sites showed that $rhaI_1$ was the strongest site and that RhaS-CTD and full-length RhaS had similar profiles for binding to the different half-sites. Finally, we demonstrated the ability of RhaS-CTD to activate transcription in vitro and further that CRP was capable of significant in vitro activation in combination with RhaS-CTD.

MATERIALS AND METHODS

Culture media and conditions. *E. coli* cultures for β-galactosidase assays were grown in MOPS (3-[*N*-morpholino]propanesulfonic acid)-buffered minimal medium using the protocol developed by Neidhardt et al. (4, 23). Tryptone broth (TB: 0.8% tryptone, 0.5% NaCl [pH 7.0]) was used to grow cultures in preparation for phage infection or transduction. $CaCl_2$ was added (final concentration, 5 mM) to tryptone broth cultures used for bacteriophage P1 infection or transduction and maltose was added (final concentration 0.2%) to tryptone broth cultures used for bacteriophage λ infection or transduction. Tryptone-yeast extract (TY) liquid medium (0.8% tryptone, 0.5% yeast extract, and 0.5% NaCl [pH 7.0]) was used to grow cells for most other experiments. All cultures were grown at 37°C. Antibiotics were used as indicated at the following concentrations: ampicillin, 200 μg/ml; chloramphenicol, 25 μg/ml; kanamycin, 25 μg/ml; and tetracycline, 20 μg/ml.

General methods, strains, and plasmids. Standard methods were used for restriction endonuclease digestion and ligation. Oligonucleotides synthesized for this study were synthesized by MWG-Biotech (High Point, NC). A list of oligonucleotides used in this study is available at http://www.molecularbiosciences.ku.edu/faculty/egan.html. The Expand high-fidelity PCR system (Roche; Indianapolis, IN) was used to amplify DNA fragments for cloning as well as to generate template DNA for sequencing of genes that were recombined onto the chromosome. DNA sequencing was performed at the Molecular Research Core Facility at Idaho State University. The DNA sequence of both strands was determined for the entire cloned region of all cloned, mutagenized, and recombined DNA fragments.

Table 1 contains the list of strains and plasmids used in this study. All strains used in β-galactosidase assays were derived from ECL116 (1). All *lacZ* fusions used in this study were translational fusions, with the exception of Φ(*rhaT-lacZ*)Δ84, which was a transcriptional fusion. The *lacZ* fusions are named such that "Φ" stands for fusion and the upstream endpoint of each fusion relative to the transcription start site (for example, −84, but without the minus sign) is given after the "Δ." The *lacZ* translational fusions were initially constructed on the plasmid pRS414, while the transcriptional fusion was constructed on pRS415 (32). The *lacZ* fusions used in all experiments, except those in Fig. 5, were then recombined onto the genome of bacteriophage λ and integrated into the bacterial chromosome as lysogens (32). Single-copy λ lysogens were identified using β-galactosidase assays and then confirmed using the Ter test (15). β-Galactosidase assays were performed using the Miller method, as previously described (4, 22). Specific activities were averaged from at least three independent assays, with two replicates in each assay. In all β-galactosidase assays, error was less than 20% of the average values.

Construction of plasmids for overexpression and purification of His_6-RhaS-CTD and His_6-RhaR-CTD proteins. The N-terminal His_6-tagged versions of RhaR-CTD and RhaS-CTD were expressed from pSE227 and pSE230, respectively. The RhaR- and RhaS-coding regions of pSE227 and pSE230 were amplified by PCR using pSE101 as the template and the following oligonucleotides: 2345 and 2346 for *rhaR* and 2349 and 2350 for *rhaS*. The PCR-amplified DNA was then ligated to pET15b using the NdeI and BamHI restriction sites such that the vector-encoded N-terminal His_6 tag was fused in frame with the RhaS- and RhaR-coding regions.

Overexpression and purification of His_6-RhaS-CTD and His_6-RhaR-CTD. All protein overexpression was performed in strain BL21(DE3) (Novagen). The cells were grown to an A_{600} of approximately 1.0, induced with 1 mM IPTG (isopropyl-β-D-thiogalactopyranoside), and incubated for an additional 3 h. After harvesting the cells, the cell pellets were resuspended in chromatography binding buffer (5 mM imidazole, 0.5 M sodium chloride, 20 mM Tris-HCl [pH 7.9]) and sonicated. After sonication, the lysate was centrifuged to separate soluble proteins from insoluble proteins. At this level of overexpression, the vast majority of the proteins were present in the insoluble, pellet fraction. Therefore, the pellet fractions from the sonication lysates were resuspended in chromatography binding buffer containing 6 M urea and rocked overnight at 4°C to solubilize the His_6-RhaS-CTD and His_6-RhaR-CTD proteins. The next day, the urea-containing suspensions were centrifuged to remove the remaining insoluble protein and the supernatant fractions were loaded onto immobilized metal affinity chromatography columns made with Ni^+-charged Chelex 20 resin (Sigma) that had been pre-equilibrated with binding buffer containing 6 M urea. The columns were washed with five volumes of binding buffer (containing 6 M urea) and then with 3 volumes of wash buffer (60 mM imidazole, 0.5 M sodium chloride, 20 mM Tris-HCl [pH 7.9]) containing 6 M urea. In order to allow refolding of the protein on the column, the columns were washed with three volumes of wash buffer without urea and the His_6-tagged proteins were then eluted with 3 volumes of elution buffer (0.5 M imidazole, 0.5 M sodium chloride, 20 mM Tris-HCl [pH 7.9]). CRP with no added His_6 tag was also purified by immobilized metal affinity chromatography, using the procedure previously described (43).

Construction of RhaS, RhaS-CTD, and RhaR-CTD expression plasmids for in vivo experiments. In order to test the ability of His_6-RhaS-CTD and His_6-RhaR-CTD to activate transcription in vivo, the respective genes were subcloned from pSE230 and pSE227 into pSU18 to make pSE271 and pSE272, respectively (using primers 2453 and 2454 in both cases). The subcloning involved digesting the PCR products with EcoRI and HindIII and then ligating them to similarly digested pSU18. In the resulting constructs, the *lac* promoter of pSU18 drives transcription and the ribosome binding site from pET15b (which was subcloned along with the open reading frame from pSE230 and pSE227) drives translation. A non-His_6-tagged version of RhaS-CTD (pSE274) in pSU18 and an equivalent version of full-length RhaS (pSE273) were also constructed by PCR amplification from pSE101 and addition of a primer-encoded Shine-Dalgarno sequence that was equivalent to the Shine-Dalgarno sequence in pET15b. The upstream

TABLE 1. Strains and plasmids used in this study

E. coli strain or plasmid	Genotype	Source or reference
Strains		
BL21(DE3)	F$^-$ *ompT gal dcm lon hsdS*$_B$ λDE3	Novagen
ECL116	F$^-$ Δ*lacU169 endA hsdR thi*	1
SME1048	ECL116 *recA*::*cat*	Laboratory collection
SME1051	ECL116 Δ*rhaSR*::*kan*	Laboratory collection
SME2986	ECL116 λΦ(*rhaB-lacZ*)Δ84 Δ*rhaSR*::*kan recA*::*cat*	This study
SME2999	ECL116 λΦ(*rhaS-lacZ*)Δ85 Δ*rhaSR*::*kan*	This study
SME3000	ECL116 λΦ(*rhaB-lacZ*)Δ84 Δ*rhaSR*::*kan*	This study
SME3066	ECL116 Δ*rhaRSBAD zih*-35::Tn*10*	This study
SME3072	ECL116 λΦ(*rhaB-lacZ*)Δ66 Δ*rhaSR*::*kan*	This study
SME3089	ECL116 λΦ(*rhaT-lacZ*)Δ84 Δ*rhaSR*::*kan*	This study
SME3114	ECL116 λΦ(*rhaB-lacZ*)Δ110 Δ*rhaSR*::*kan recA*::*cat*	This study
Plasmids		
pBluescript II SK	Ap^r *lacZ*α	Stratagene
pET15b	Ap^r *lacI* (ColE1 origin from pBR322)	Novagen
pHG165	*lacZ*α *rop* Ap^r (ColE1 origin from pBR322)	34
pRS414	*lac′ZYA*	32
pSE101	pTZ 18R Ap^r *′rhaTrhaSRrhaBA′*	Laboratory collection
pSE227	pET15b *rhaR*$_{196–312}$ (encodes N-terminal His$_6$-tagged RhaR residues 196 through 312)	This study
pSE230	pET15b *rhaS*$_{163–278}$ (encodes N-terminal His$_6$-tagged RhaS residues 163 through 278)	This study
pSE250	pUC18 *rhaSRrhaT′* wild type	This study
pSE262	pHG165 + pSR^{con} promoter	This study
pSE265	pSE262 *rhaS*	This study
pSE268	pSE262 *rhaS*$_{163–278}$ (encodes RhaS-CTD)	This study
pSE271	pSU18 *rhaS*$_{163–278}$ (encodes His$_6$-tagged RhaS-CTD from *lac* promoter)	This study
pSE272	pSU18 *rhaR*$_{196–312}$ (encodes His$_6$-tagged RhaR-CTD from *lac* promoter)	This study
pSE273	pSU18 *rhaS*	This study
pSE274	pSU18 *rhaS*$_{163–278}$ (encodes RhaR-CTD)	This study
pSE276	pRS414 Φ(*rhaB-lacZ*)Δ66	This study
pSE283	pTS134 with *rhaBAD* Δ110 promoter replacing *rhaSR* promoter	This study
pSU18	*lacZ*α Cm^r (P15A *ori*)	3
pTS134	pBluescript II SK *rhaSR* promoter	44
pUC18	Ap^r *lacZ*α	47

primers were 2571 for RhaS and 2574 for RhaS-CTD, and the downstream primer was 2542 in both cases.

Plasmid pSE262 was constructed by adding a constitutive promoter to pHG165. The inserted promoter in pSE262 (pSR^{con}) is the core *rhaSR* promoter, except the −35 hexamer was changed so that it matches the consensus −35 hexamer sequence (therefore, the −35 sequence is TTGACA, and the −10 sequence is TACTAT). Also, pSE262 has a Shine-Dalgarno sequence (GAA GGA) followed immediately by a BamHI site. Placement of a translational start codon immediately downstream of the BamHI site provides the correct spacing relative to the Shine-Dalgarno sequence for ribosome recognition. The *rhaS* gene and the gene encoding RhaS-CTD were amplified by PCR from pSE250 with primers 2731 or 2732 and 2542 and ligated to pSE262 to make pSE265 and pSE268, respectively.

Western blots to compare in vivo expression of His$_6$-RhaS-CTD and His$_6$-RhaR-CTD. To compare His$_6$-RhaS-CTD expression to His$_6$-RhaR-CTD expression in vivo, cultures of the strains used in β-galactosidase assays (Table 2) were grown to mid-log phase in TB with chloramphenicol. Cells were sedimented and resuspended in TB to identical cell densities (using A_{600}). Five hundred microliters of each sample was sonicated and separated into soluble and insoluble fractions by centrifugation. The insoluble pellets were resuspended in 500 μl TB. The total protein concentration in each sample was determined by Bradford (6) protein assay (Bio-Rad, Hercules, CA). Soluble fractions were standardized to identical protein concentrations, as were insoluble fractions, with insoluble fractions generally containing approximately 10-fold less protein than soluble fractions (the same ratio found before the minor adjustments to standardize protein concentrations). The samples were then analyzed using Western blots. Equal amounts of protein from the standardized His$_6$-RhaS-CTD- and His$_6$-RhaR-CTD-containing cell fractions were loaded onto two 15% sodium dodecyl sulfate-polyacrylamide gels, electrophoresed, and blotted onto a nitrocellulose membrane using standard procedures. We also loaded known amounts of either purified His$_6$-RhaS-CTD or His$_6$-RhaR-CTD on the gels to allow for quantification of His$_6$-RhaS-CTD or His$_6$-RhaR-CTD present in the soluble and insoluble fractions of each sample. We added total lysate from the vector-only sample (collected before fractionation) to the samples with purified protein to prevent

TABLE 2. Transcription activation by His$_6$-RhaS-CTD and His$_6$-RhaR-CTD

Promoter fusion[a]	β-Galactosidase sp act (Miller units)[b]		His$_6$-RhaS-CTD or His$_6$-RhaR-CTD activation (fold)[c]
	Vector only	His$_6$-RhaS-CTD or His$_6$-RhaR-CTD	
Φ(*rhaB-lacZ*)Δ84	0.021	21 (His$_6$-RhaS-CTD)	1,000 (His$_6$-RhaS-CTD)
Φ(*rhaT-lacZ*)Δ84[d]	0.29	51 (His$_6$-RhaS-CTD)	180 (His$_6$-RhaS-CTD)
Φ(*rhaS-lacZ*)Δ85	0.41	0.82 (His$_6$-RhaR-CTD)	2.0 (His$_6$-RhaR-CTD)

[a] Each strain carried a single-copy *lacZ* fusion integrated into the chromosome as a λ lysogen and also Δ(*rhaSR*).
[b] β-Galactosidase activity was determined as described in Materials and Methods. The vector-only sample was pSU18. His$_6$-RhaS-CTD was expressed from pSE271, and His$_6$-RhaR-CTD was expressed from pSE272.
[c] Activation values (fold) were calculated by dividing the activity in the presence of His$_6$-RhaS-CTD or His$_6$-RhaR-CTD by the activity in the presence of vector only.
[d] Φ(*rhaT-lacZ*)Δ84 is a transcriptional fusion. All other *lacZ* fusions in this study were translational fusions.

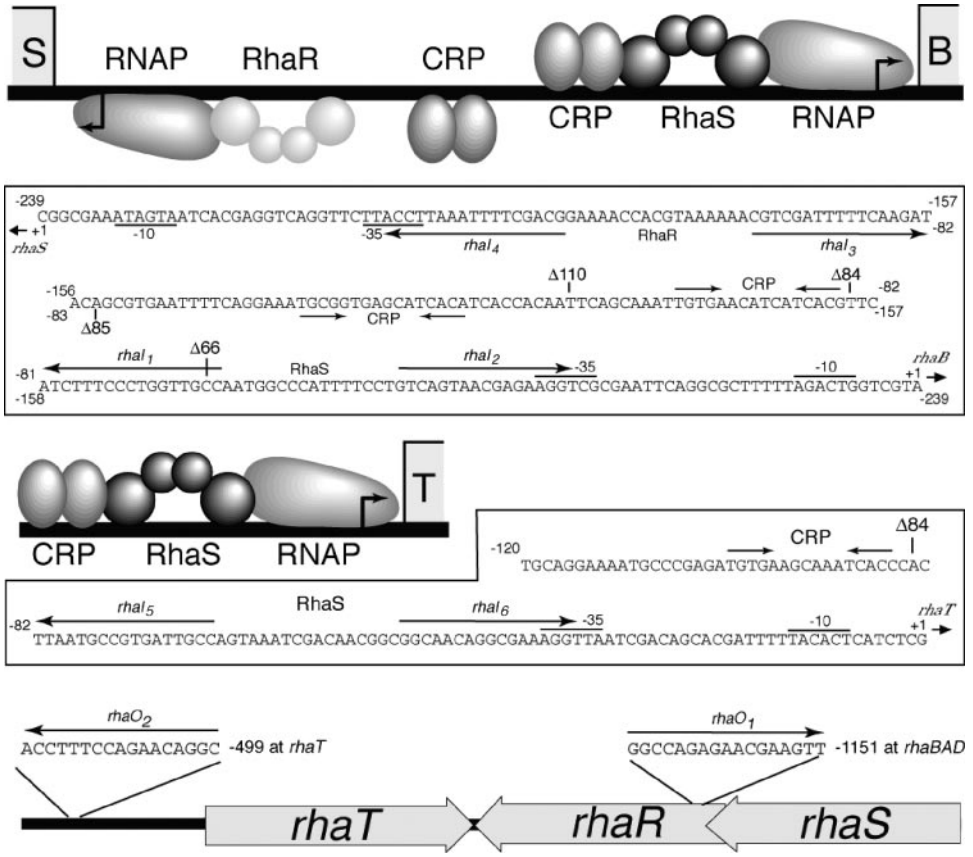

FIG. 1. RhaS and RhaR binding sites within the L-rhamnose regulon. For each promoter (*rhaSR*, *rhaBAD*, and *rhaT*), there is a schematic showing the known proteins and binding sites and below each schematic is the DNA sequence of that promoter region. Within the *rhaSR-rhaBAD* intergenic region, labels for the *rhaSR* promoter are below the DNA sequence and labels for the *rhaBAD* promoter are above the DNA sequence. The upstream endpoints of the *lacZ* fusions used in this study (in bp upstream from the transcription start site) are indicated with Δ. The RhaS and RhaR binding sites are shown as half-sites and labeled with the half-site number ($rhaI_x$). The orientation of each half-site is indicated with an arrow. RhaS (dark gray) and RhaR (light gray) are depicted as dimers, with each monomer consisting of two domains, a C-terminal DNA-binding domain and an N-terminal dimerization domain, depicted as spheres. The bottom figure shows the approximate positions of the *rhaO* half-sites (which are outside of the promoter regions) within the L-rhamnose region.

differences in antibody-antigen binding due to the lack of other proteins in the sample. The primary antibodies (anti-RhaS and anti-RhaR) were custom-made polyclonal rabbit antibodies from Cocalico Biologicals (Reamstown, PA). Anti-RhaS antibody was preadsorbed against a lysate of strain SME3066 (Δ*rhaRSBAD*) in order to remove rabbit antibodies to other *E. coli* proteins. This preadsorption step was not necessary for anti-RhaR antibody. The Alexa Fluor 680-labeled secondary antibody (anti-rabbit) was obtained from Molecular Probes (Eugene, OR). The blots were imaged using an Odyssey Infrared Imaging System (LI-COR, Lincoln, NE).

DNase I footprinting. The template DNAs for DNase I footprinting were generated by PCR using the following templates and primers: *rhaBAD* was amplified from pSE101 using primers 2371 and 2410, *rhaT* was amplified from ECL116 cells using primers 2096 (^{32}P-labeled) and 2097 for one strand and primers 2655 (^{32}P-labeled) and 2656 for the other strand, and *rhaSR* was amplified from pSE101 using primers 2371 and 2409. DNase I footprinting was performed as previously described (44). Gels were imaged by autoradiography. In addition to the results shown, similar results were obtained when the other DNA strand was labeled. All DNase I footprinting experiments were carried out at least twice.

Construction of *rhaI* half-site fusions on plasmids. The half-site fusions used to compare the strengths of various RhaS DNA half-sites were constructed in the context of a Φ(*rhaB-lacZ*)Δ66 fusion (Fig. 1) in pRS414. At the wild-type *rhaBAD* promoter, the $rhaI_2$ half-site overlaps the −35 hexamer of RNAP by 4 bp. The other RhaS half-sites were placed in the position of $rhaI_2$; however, the DNA sequence of the 4-bp overlap with the −35 hexamer was not changed (Fig. 5C). (Constructs in which the −35 sequence was changed to match that of the $rhaI_1$, $rhaI_5$, and $rhaO_1$ half-site resulted in extremely low expression [unpublished results].) The DNA sequence surrounding each half-site was identical in every case. The wild-type Φ(*rhaB-lacZ*)Δ66 fusion (pSE276) was created by PCR with oligonucleotides 2414 and 744, using pSE101 as the template. The other half-site fusions were constructed by PCR using an oligonucleotide-encoded half-site in the upstream primer (2413, 2441, 2442, 2445, and 2446) and oligonucleotide 744 downstream, and the resulting plasmids were named pSE276 $rhaI_X$ (where "X" represents the half-site number).

In vitro transcription assays. Single-round in vitro transcription assays were carried out with core RNAP and σ^{70} purified as described previously (48, 49). Reconstitution of σ^{70} with core RNAP was carried out by mixing 4 μg core RNAP and 0.7 μg σ^{70} (1:1 molar ratio) in 100 μl of RNAP storage buffer (50 mM Tris-HCl [pH 8.0], 50% glycerol, 0.1 mM NaEDTA, 0.1 mM dithiothreitol, 50 mM NaCl), incubating the mixture at 25°C for 10 min, and then storing it at −20°C. To prepare the transcription reaction, His_6-RhaS-CTD and/or CRP was incubated with *rhaBAD* promoter template DNA (PCR amplified with oligonucleotides 744 and 2654) in IVT reaction buffer (final concentrations in reaction mixture, 20 mM Tris-HCl [pH 7.9], 50 mM KCl, 4 mM $MgCl_2$, 1 mM dithiothreitol, 0.1 mM KEDTA, 0.1 mg/ml bovine serum albumin, 50 mM L-rhamnose, 0.2 mM cAMP) at 37°C for 10 min. RNAP was then added (10 nM final concentration), and the reaction mixture was incubated for 5 min at 37°C. An initiation mixture was added (final concentrations in reaction mixture, 0.2 mM each ATP, CTP, and GTP; 0.02 mM UTP; 100 mg/ml heparin; 0.2 μCi [α-^{32}P]UTP [3,000 Ci/mmol]). The reaction mixture was next incubated at 37°C for 10 min, and then the reaction was stopped by addition of 0.25 volume of stop solution (7 M urea, 0.1 M KEDTA, 0.4% sodium dodecyl sulfate, 20 mM

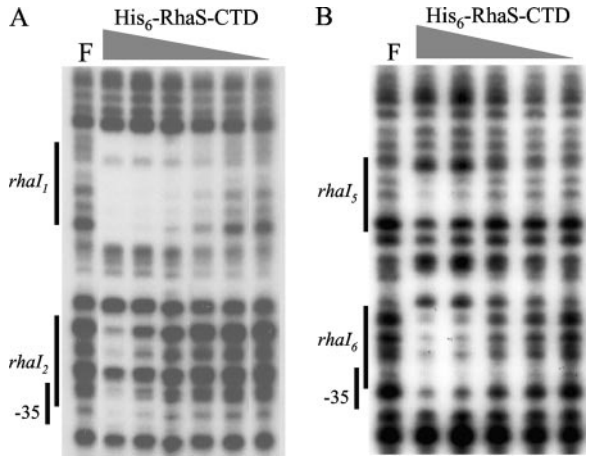

FIG. 2. DNase I footprinting assay of His_6-RhaS-CTD binding to the *rhaBAD* promoter (A) and the *rhaT* promoter (B). The DNA fragment used as the template for *rhaBAD* was generated by PCR with primers 2371 (^{32}P labeled) and 2410, while that for *rhaT* was generated with primers 2096 (^{32}P labeled) and 2097. The positions of the RhaS half-sites were determined based on a DNA sequencing ladder (not shown). The highest His_6-RhaS-CTD concentration was 6 μM, and the dilution steps were threefold. F, free DNA.

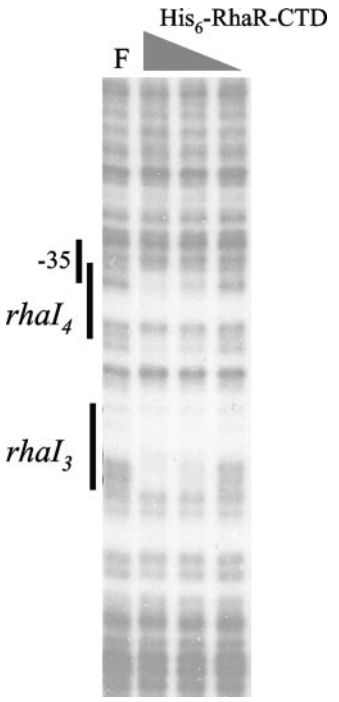

FIG. 3. DNase I footprinting assay of His_6-RhaR-CTD binding to the *rhaSR* promoter. The DNA fragment used as the template was generated by PCR with primers 2371 (^{32}P labeled) and 2409. The positions of the RhaR half-sites were determined based on a DNA sequencing ladder (not shown). The highest His_6-RhaR-CTD concentration was 5 μM, and the dilution steps were threefold. F, free DNA.

Tris-HCl [pH 7.9], 0.5% bromophenol blue, 0.5% xylene cyanol). The reaction mixture was then loaded directly onto a preheated 6% denaturing polyacrylamide gel for electrophoresis (0.3% *N*,*N*-methylenebisacrylamide, 8.9 mM Tris, 8.9 mM boric acid, 20 mM EDTA, 8 M urea). The gels were imaged and analyzed using a Cyclone storage phosphor system (Perkin-Elmer). The results shown are representative of three similar experiments.

RESULTS

In vitro DNA binding by His_6-RhaS-CTD and His_6-RhaR-CTD. Specific residues in the CTDs of RhaS and RhaR had previously been shown to contribute to DNA binding and transcription activation (4, 5, 38, 42). In order to test whether the CTD of each protein was sufficient for DNA binding and transcription activation, we constructed plasmids expressing truncated versions of RhaS (encoding His_6-RhaS-CTD, consisting of RhaS amino acids 163 to 278), and RhaR (encoding His_6-RhaR-CTD, consisting of RhaR amino acids 196 to 312). We tested the in vitro DNA-binding activity of His_6-RhaS-CTD and His_6-RhaR-CTD by performing DNase I footprinting using the purified proteins. We found that His6-RhaS-CTD bound to the *rhaBAD* promoter region at two sites (Fig. 2A). The extent of the two footprinted regions corresponds very well with the two half-sites for RhaS binding previously predicted from the footprint of full-length RhaS and mutagenesis of the binding site region (12). There were two differences from the previously published footprints; however, both were consistent with the prediction that His_6-RhaS-CTD is monomeric, whereas full-length RhaS is dimeric. First, His_6-RhaS-CTD did not protect the DNA between the two half-sites, while full-length RhaS did. Second, it was possible to observe differences in the binding strengths to the two half-sites with His_6-RhaS-CTD. We found that there were protein concentrations at which the footprint at $rhaI_1$ (the promoter distal half-site) was detectable while the footprint at $rhaI_2$ (the promoter proximal half-site) was no longer detectable, indicating that His_6-RhaS-CTD bound more tightly to $rhaI_1$ than to $rhaI_2$ (Fig. 2A).

We also performed DNase I footprinting with His_6-RhaS-CTD at the *rhaT* promoter. DNA sequence inspection and previous results indicating that RhaS was required for activation of *rhaT* expression (40) suggested that RhaS binds to DNA at the *rhaT* promoter, but direct evidence of RhaS protein binding to *rhaT* promoter DNA had not been obtained. Our DNase I footprinting results provide direct evidence of His_6-RhaS-CTD binding to the predicted RhaS half-sites at the *rhaT* promoter (Fig. 2B). In this case, His_6-RhaS-CTD appeared to have a slightly higher affinity for the $rhaI_6$ half-site (the promoter-proximal half-site) than the $rhaI_5$ half-site (the promoter distal half-site). While the protection of $rhaI_5$ was weak, we were unable to use higher protein concentrations in this experiment due to the tendency of His_6-RhaS-CTD to aggregate.

Finally, we tested in vitro DNA binding by His_6-RhaR-CTD by DNase I footprinting. We found that His_6-RhaR-CTD showed specific binding to two sites within *rhaSR* promoter DNA (Fig. 3). There was somewhat more ambiguity than usual in the exact extent of the protected regions in this case due to the relative lack of DNase I cleavage sites within the A tracts, especially in the region of $rhaI_3$; however, the two protected regions appear to correspond well with the previously demonstrated RhaR half-sites (38, 44). There was not any substantial difference in the apparent strength of His_6-RhaR-CTD binding to the two half-sites. These results indicate that our purified His_6-RhaS-CTD and His_6-RhaR-CTD protein preparations

contained active proteins that were capable of specifically binding to DNA.

The CTD of RhaS but not RhaR is sufficient for transcription activation. His_6-RhaS-CTD was tested for in vivo activation of *lacZ* fusions to the *rhaBAD* and *rhaT* promoters, while His_6-RhaR-CTD was tested for in vivo activation of a *lacZ* fusion to the *rhaSR* promoter (Fig. 1). We found that plasmid-expressed His_6-RhaS-CTD could activate transcription to high levels, with 1,000-fold activation of the *rhaBAD* promoter and 180-fold activation of the *rhaT* promoter (Table 2). In contrast, plasmid-expressed His_6-RhaR-CTD could only activate expression of the *rhaSR* promoter by twofold (Table 2). Given that the activation by full-length, chromosomally expressed RhaS at *rhaBAD* is approximately 33-fold higher than that of chromosomally expressed RhaR at *rhaSR*, comparable efficiencies of activation by the CTDs to their full-length counterparts would have resulted in His_6-RhaR-CTD activating *rhaSR* by approximately 30-fold. This value is much higher than the twofold value measured for His_6-RhaR-CTD. To test whether the very poor activation might be due to an artifact of our His_6-RhaR-CTD-expressing construct, we made a number of different RhaR-CTD constructs; however, none were capable of significant transcription activation. Our results suggest that although His_6-RhaR-CTD is capable of specific DNA binding, it is not capable of activating transcription well. Interestingly, Tobin and Schleif previously found that in the absence of L-rhamnose, full-length RhaR was able to bind to DNA but was not able to activate transcription (38, 39), suggesting that His_6-RhaR-CTD (which lacks an L-rhamnose-binding domain) may be similar in its activity to full-length RhaR in the absence of L-rhamnose.

To test whether the low level of activation by His_6-RhaR-CTD could be due to a low level of His_6-RhaR-CTD protein expression or stability compared with the His_6-RhaS-CTD protein, we performed Western blots with samples of the same strains assayed in Table 2. We found that both soluble His_6-RhaS-CTD (Fig. 4, top blot, lane 3) and soluble His_6-RhaR-CTD (Fig. 4, bottom blot, lane 5) were present in substantial amounts, based on comparisons with known amounts of the respective purified proteins. However, soluble His_6-RhaS-CTD (5.5 ng/μg of soluble protein) was present at a level approximately 5.5-fold higher than that of soluble His_6-RhaR-CTD (1.0 ng/μg of soluble protein). This 5.5-fold difference in soluble protein levels could explain some of the decrease in activation by His_6-RhaR-CTD at *rhaSR* relative to His_6-RhaS-CTD at *rhaBAD*; however, the similarity in the activity of His6-RhaR-CTD to that of full-length RhaR in the absence of L-rhamnose suggests that His_6-RhaR-CTD may simply be unable to activate transcription well. Our results also showed that His_6-RhaS-CTD and His_6-RhaR-CTD did not respond to L-rhamnose availability (data not shown), which was expected since, based on sequence similarity with AraC, L-rhamnose binding is predicted to be a function of the RhaS and RhaR N-terminal domains.

Comparison of RhaS and RhaS-CTD activation of *rhaB-lacZ* fusions. The above results (Table 2) indicate that RhaS-CTD was capable of activating transcription from a *rhaB-lacZ* fusion that includes the full RhaS binding site. We next tested whether both or only one of the RhaS half-sites contribute to RhaS-CTD activation and whether RhaS-CTD is sufficient to allow CRP to contribute to *rhaBAD* activation. Given that it lacks its dimerization domain, we predicted that RhaS-CTD would function as a monomer, similar to MarA (28). We expected that the RhaS-CTD monomer that bound to the half-site adjacent to RNAP would contribute to transcription activation based on our previous finding that RhaS contacts with σ^{70} contribute to transcription activation (5, 42). We also have some evidence that activation by RhaS may involve contacts with α-CTD (17); therefore, it was possible that RhaS-CTD bound to the promoter-distal RhaS half-site might further contribute to transcription activation. Previous in vivo experiments also indicate that CRP is not capable of activating *rhaBAD* expression in the absence of RhaS (11), perhaps suggesting that RhaS must bend the DNA to allow CRP to activate, although other possibilities exist as well. Therefore, we also tested whether RhaS-CTD was capable of fulfilling the function of RhaS that allows CRP activation.

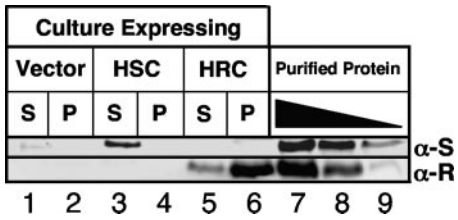

FIG. 4. Western blots comparing in vivo levels of expression of His_6-RhaS-CTD and His_6-RhaR-CTD. Soluble (S, supernatant) and insoluble (P, pellet) fractions after sonication were loaded as indicated. The vector-only sample was pSU18. His_6-RhaS-CTD (HSC) was expressed from pSE271, and His_6-RhaR-CTD (HRC) was expressed from pSE272. Lanes 7 to 9 on each gel contained known amounts of purified His_6-RhaS-CTD (top blot) or His_6-RhaR-CTD (bottom blot). The amounts of His_6-RhaS-CTD were 737 (lane 7), 368 (lane 8), and 184 (lane 9) ng. The amounts of His_6-RhaR-CTD were 162 (lane 7), 54 (lane 8), and 18 (lane 9) ng. Two gels were prepared, with identical culture samples on each gel, and each blot was probed with the primary antibody corresponding to the purified protein samples loaded, as indicated to the right. α-S, anti-RhaS antibody; α-R, anti-RhaR antibody.

To address these questions, we compared transcription activation by full-length RhaS and RhaS-CTD (no His_6 tag) at three different truncations of the *rhaBAD* promoter (each fused to *lacZ* and carried as a single-copy λ lysogen) (Fig. 1). At Φ(*rhaB-lacZ*)Δ66, which carries only one half-site of the full RhaS binding site, RhaS-CTD was capable of more than 2,000-fold activation (Table 3). Interestingly, this was a 10-fold-higher level than when similarly expressed full-length RhaS activated this fusion. At the Φ(*rhaB-lacZ*)Δ84 fusion, which carries the full RhaS binding site, there was no increase in the activation by RhaS-CTD, indicating that RhaS-CTD activation occurs from the promoter proximal half-site and consistent with the prediction that RhaS-CTD functions as a monomer. In contrast, full-length RhaS activated this fusion to a level more than 30-fold higher than its activation of the fusion containing only a single RhaS half-site and 3-fold higher than the activation by RhaS-CTD. Finally, at the Φ(*rhaB-lacZ*)Δ110 fusion, which contains the CRP site required for full *rhaBAD* activation as well as the full RhaS binding site, there was a twofold contribution to activation by CRP when in combination with RhaS-CTD and a fivefold contribution to activation

TABLE 3. Transcription activation by RhaS-CTD compared to full-length RhaS

Promoter fusion[a]	β-Galactosidase sp act (Miller units)[b]			Activation (fold) with:[c]	
	Vector	RhaS-CTD	RhaS	RhaS-CTD	RhaS
Φ(*rhaB-lacZ*)Δ66	0.015	34	3.5	2,300	230
Φ(*rhaB-lacZ*)Δ84	0.015	36	110	2,400	7,300
Φ(*rhaB-lacZ*)Δ110	0.018	91	700	5,100	39,000

[a] Each strain carried a single-copy *lacZ* fusion integrated into the chromosome as a λ lysogen and also Δ(*rhaSR*).

[b] β-Galactosidase activity was determined as described in Materials and Methods. All cultures were grown in the presence of L-rhamnose. The vector-only sample was pSE262. RhaS-CTD was expressed from pSE268, and RhaS was expressed from pSE265.

[c] Activation (fold) values were calculated by dividing the activity in the presence of RhaS-CTD or RhaS by the activity in the presence of vector only.

by CRP when in combination with full-length RhaS. This suggests that RhaS-CTD can fulfill at least part of the function of RhaS that allows CRP activation at *rhaBAD*.

In vivo comparison of different RhaS half-sites. The DNase I footprinting assays indicated that there were differences in the relative strengths of the RhaS half-sites at the *rhaBAD* and *rhaT* promoters. In order to further compare RhaS binding to the RhaS half-sites, each half-site was placed at the same position in the context of the Φ(*rhaB-lacZ*)Δ66 promoter (referred to as "half-site fusions"). In these constructs, each of the half-sites replaces $rhaI_2$, the wild-type promoter-proximal half-site, at this promoter (Fig. 1). In addition to the four previously identified RhaS half-sites, we also tested two additional DNA sequences that were identified using a string-matching program (written in the computer language Perl) to identify potential RhaS half-sites within the entire *rha* region. The program identified only two DNA sequences with perfect matches in sequence and spacing to the 6 bp previously identified as most important for RhaS binding (12) (Fig. 5C). One of the potential half-sites ($rhaO_1$) is located within the *rhaR* gene and is centered at −1153 relative to the *rhaBAD* transcription start site or at +914 relative to the *rhaSR* transcription start site, while the other potential site ($rhaO_2$) is centered at −499 relative to the *rhaT* transcription start site.

We first tested the ability of each of the half-site fusions to be activated in vivo by His_6-RhaS-CTD (Fig. 5A). Among the previously identified RhaS half-sites, we found the greatest activation (fold) at $rhaI_1$, followed by $rhaI_6$, then $rhaI_2$, and finally $rhaI_5$. These results confirm the relative half-site strengths identified by DNase I footprinting and further provide information about the relative strengths of the *rhaBAD* versus *rhaT* half-sites. We also found that His_6-RhaS-CTD could activate transcription from the fusion carrying the $rhaO_1$ half-site to an extent comparable with that of the previously identified half-sites, while there was only a very low level of activation from $rhaO_2$. The same order of relative half-site strengths was also determined using electrophoretic mobility shift assays with purified His_6-RhaS-CTD (data not shown). The ability of His_6-RhaS-CTD to activate transcription to a high level from $rhaO_1$ confirms that the 6 bp used to identify this site are important for RhaS binding; however, the low level of activation with $rhaO_2$ suggests that the context of these 6 bp is also important. We also tested the same set of half-site fusions for activation by full-length RhaS expressed from the chromosome (Fig. 5B). We found a very similar order of apparent half-site strengths in this experiment, although the position of $rhaI_2$ in the order was different and the magnitude of activation by RhaS from these fusions was much lower than that by His_6-RhaS-CTD. In this case, there was no activation

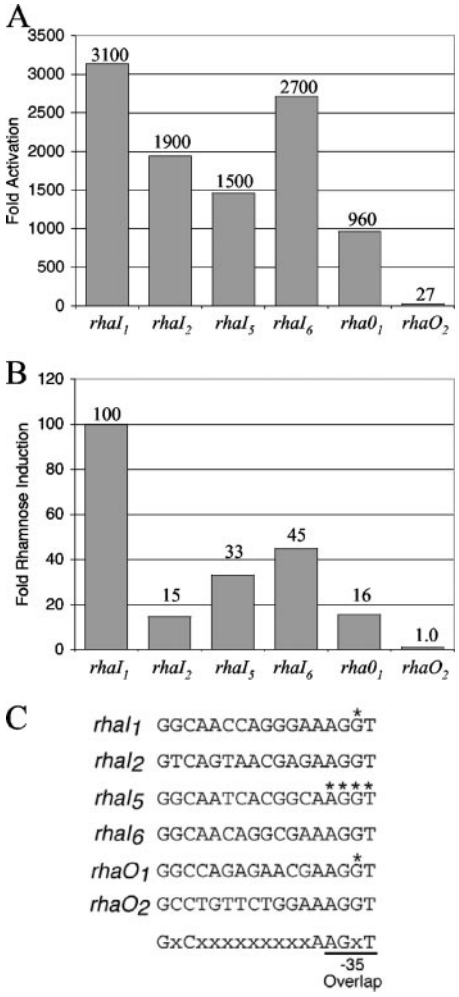

FIG. 5. In vivo transcription activation by His_6-RhaS-CTD or RhaS. The indicated RhaS half-sites, in the context of Φ(*rhaB-lacZ*)Δ66 on multicopy plasmids (pSE276 and derivatives), were assayed for β-galactosidase activity. Cells were grown in TY medium. (A) Activation by His_6-RhaS-CTD, expressed from pSE271 in SME1051 [Δ(*rhaSR*)]. Activation (fold) was determined by dividing the activity obtained with RhaS-CTD by the activity of pSU18 alone (vector only) at each promoter. The activity of pSU18 alone ranged from 0.39 to 0.99 Miller units. (B) Transcription activation by RhaS expressed from the chromosome in SME1048 (wild-type *rhaSR*). Rhamnose induction (fold) was determined by dividing the activity of each fusion in the presence of rhamnose by the activity of the same fusion in the absence of rhamnose. The activities in the absence of rhamnose ranged from 0.21 to 0.29 Miller units. (C) The DNA sequences of the half-sites used in these experiments are shown. The asterisks indicate positions at which base pairs were changed from the wild-type half-site sequences (see Fig. 1) so that the DNA sequence of the overlapping −35 element was not changed. The bottom line indicates the sequence and position of the 6 important bp in the RhaS binding site that were used to identify $rhaO_1$ and $rhaO_2$.

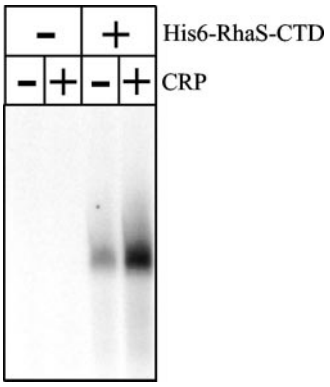

FIG. 6. In vitro transcription activation by His_6-RhaS-CTD. The linear template DNA containing the *rhaBAD* promoter was generated by PCR using primers 744 and 2654 with pSE283 as the template. When present (as indicated above the gel), the His_6-RhaS-CTD concentration was 10 μM and the CRP concentration was 1 μM. cAMP was present in all reactions.

from the $rhaO_2$ half-site, further supporting the idea that it is, at best, a marginal RhaS half-site.

Transcription activation by His_6-RhaS-CTD in vitro. Given that RhaS-CTD (both with and without a His_6 tag) was capable of activating transcription in vivo and was capable of specifically binding to DNA at RhaS half-sites in vitro, we investigated its ability to activate transcription in a purified in vitro transcription assay. We have never been able to carry out in vitro transcription with full-length RhaS due to its insolubility. In preliminary experiments, we found that His_6-RhaS-CTD activated transcription much more efficiently from linear DNA templates than from supercoiled DNA templates (data not shown), in contrast to full-length RhaR, which required supercoiled DNA templates for efficient in vitro transcription activation (39, 44). We found that CRP alone was not capable of activating *rhaBAD* expression, similar to previous findings in vivo, and that His_6-RhaS-CTD alone substantially activated *rhaBAD* expression (Fig. 6). We also found that CRP and His_6-RhaS-CTD together could activate transcription to a level that was threefold higher than that by His_6-RhaS-CTD alone. The threefold contribution to activation by CRP in this experiment is very similar to the twofold contribution found in the above in vivo experiment (Table 3), confirming that RhaS-CTD is sufficient to allow at least partial CRP activation of *rhaBAD* expression. This in vitro transcription system mimics the in vivo activation of *rhaBAD* by RhaS-CTD and also, to a great extent, the in vivo activation of *rhaBAD* by full-length RhaS, each in the presence and absence of CRP. Consistent with the very low level of activation in our in vivo results, we were not able to detect transcription activation by His_6-RhaR-CTD (data not shown).

DISCUSSION

In vivo transcription activation by RhaS-CTD. Our results indicate that RhaS-CTD (with and without a His_6 tag) could activate transcription very well and that purified His_6-RhaS-CTD protein was able to bind to DNA at the previously identified or predicted RhaS half-sites at *rhaBAD* and *rhaT*. Based on the amino acid sequence alignment of RhaS with AraC, as well as our studies of RhaS (Kolin and Egan, unpublished), we predicted that the dimerization interface of RhaS would be located in its NTD. Several pieces of evidence in this study are consistent with the prediction that RhaS-CTD functions as a monomer. His_6-RhaS-CTD did not footprint the DNA between the two RhaS half-sites, nor did binding by His_6-RhaS-CTD exhibit much if any cooperative binding to the two half-sites at *rhaBAD* and *rhaT*, in both cases, unlike full-length RhaS (12). The level of transcription activation by RhaS-CTD also did not increase with the addition of a second RhaS half-site, again unlike full-length RhaS.

We were also not surprised to find that RhaS-CTD was capable of equivalent transcription activation in the absence and the presence of L-rhamnose (data not shown), since amino acid sequence alignment with AraC suggests that the RhaS N-terminal domain likely binds L-rhamnose. The differential activation of transcription by full-length RhaS in the absence and presence of L-rhamnose could be due either to inhibition of activity in the absence of ligand or stimulation of activity in the presence of ligand. The finding that RhaS-CTD activates transcription very well in the absence of RhaS-NTD suggests that there may be inhibition of full-length RhaS activity in the absence of ligand. The light-switch mechanism used by AraC to respond to its ligand arabinose also involves inhibition in the absence of ligand (14, 27, 29, 31, 45, 46). However, our more recent results suggest that the L-rhamnose response of RhaS most likely involves an active stimulation of activity in the presence of L-rhamnose (Kolin and Egan, unpublished [see below]).

In vitro DNA binding and transcription activation by His_6-RhaS-CTD. We found that purified His_6-RhaS-CTD was capable of specific DNA binding and also activation of transcription in purified in vitro reactions. Prior to this work, in vitro studies of the L-rhamnose regulon have been severely hampered by the strong tendency of full-length RhaS to aggregate. Our only previously published in vitro studies involving RhaS utilized partially purified protein that was refolded on a "per-reaction" basis in the presence of specific DNA (12). We have never been able to obtain full-length RhaS that is both soluble and active by refolding of protein purified under denaturing conditions nor by fusion with proteins that promote solubility. Therefore, our finding that His_6-RhaS-CTD is capable of both specific DNA binding and activation of transcription in vitro represents a major breakthrough in our studies of the L-rhamnose regulon. While His_6-RhaS-CTD is not entirely free of aggregation problems, its aggregation is substantially more manageable than that of full-length RhaS.

RhaS-CTD binding to *rhaI* half-sites. Our DNase I footprinting and in vivo transcription assays both indicated that His_6-RhaS-CTD bound to the $rhaI_1$ half-site at *rhaBAD* significantly more strongly than to the $rhaI_2$ half-site. This finding is similar to previous findings with the AraC and MelR proteins in which the activator binds to its upstream half-site much more tightly than its downstream half-site (8, 9, 18, 31) and in the absence of ligand forms a DNA loop that represses transcription (30, 41). To begin to address the question of whether RhaS regulation might involve DNA looping, we used a bioinformatics approach to look for other potential RhaS half-sites in the *rha* region. One of the two sites we identified, $rhaO_1$, is

located within the *rhaR* gene at −1153 relative to the *rhaBAD* transcription start site or +914 relative to the *rhaSR* transcription start site. The finding that RhaS binds to $rhaO_1$ with an apparent strength that is comparable to that of the known RhaS half-sites suggests the possibility that it has some in vivo function, although whether there is a role and whether that role might involve DNA looping remain to be determined.

Differences between RhaS-CTD and RhaR-CTD. Given that RhaS-CTD and RhaR-CTD share 34% amino acid sequence identity, we were surprised to find that His_6-RhaS-CTD efficiently activated transcription, while His_6-RhaR-CTD only barely activated transcription. Although the presence of low protein levels may partially account for the lower activation by His_6-RhaR-CTD, we would argue it is not the full explanation. Purified His_6-RhaR-CTD protein was capable of binding to DNA, indicating that this fusion protein contained the necessary determinants for DNA binding and was capable of folding correctly. One hypothesis to explain the very low activation by His_6-RhaR-CTD might be that its DNA-binding motifs are correctly folded but that its transcription activation determinants are not properly folded. This hypothesis seems highly unlikely given that RhaR residue D276 is located within the stabilizing helix of one of the HTH DNA-binding motifs and that this σ^{70}-contacting residue is responsible for approximately two-thirds of the transcription activation by RhaR (42). Also, as mentioned above, Tobin and Schleif (38, 39) previously found that, similar to His_6-RhaR-CTD, full-length RhaR in the absence of L-rhamnose was capable of binding to DNA but not capable of activating transcription. It seems likely, therefore, that RhaR-CTD requires a signal from RhaR-NTD in the presence of L-rhamnose in order to activate transcription and therefore is unable to activate in the absence of RhaR-NTD. RhaS, therefore, provides an additional example of an AraC/XylS family protein whose DNA-binding domain is capable of efficient transcription activation in the absence of a second domain. In contrast, RhaR may be an additional example of an AraC/XylS family protein whose DNA-binding domain alone is capable of little or no transcription activation.

ACKNOWLEDGMENTS

We would like to thank Peter Gegenheimer for use of his Cyclone storage phosphor system and members of the laboratory of William Picking, especially Marianela Espina and Andrew Olive, for help with Western blots and image analysis. Western blot images were obtained on an Odyssey Infrared Imager through collaboration with LI-COR, Inc.

This work was supported by NIH grant GM55099 from the National Institute of General Medical Sciences and NIH grant P20 RR17708 from the Institutional Development Award (IDeA) Program of the National Center for Research Resources (both to S.M.E.), NIH grant P20 RR016475 (to J.F.), and the Intramural Research Program of NIH, National Cancer Institute, Center for Cancer Research (to D.J.J.).

REFERENCES

1. **Backman, K., Y.-M. Chen, and B. Magasanik.** 1981. Physical and genetic characterization of the *gln A-glnG* region of the *Escherichia coli* chromosome. Proc. Natl. Acad. Sci. USA **78:**3743–3747.
2. **Badia, J., L. Baldoma, J. Aguilar, and A. Boronat.** 1989. Identification of the *rhaA*, *rhaB* and *rhaD* gene products from *Escherichia coli* K-12. FEMS Microbiol. Lett. **65:**253–258.
3. **Bartolome, B., Y. Jubete, E. Martinez, and F. de la Cruz.** 1991. Construction and properties of a family of pACYC184-derived cloning vectors compatible with pBR322 and its derivatives. Gene **102:**75–78.
4. **Bhende, P. M., and S. M. Egan.** 1999. Amino acid-DNA contacts by RhaS: an AraC family transcription activator. J. Bacteriol. **181:**5185–5192.
5. **Bhende, P. M., and S. M. Egan.** 2000. Genetic evidence that transcription activation by RhaS involves specific amino acid contacts with sigma 70. J. Bacteriol. **182:**4959–4969.
6. **Bradford, M. M.** 1976. A rapid and sensitive method for the quantitation of microgram quantities of protein utilizing the principle of protein-dye binding. Anal. Biochem. **72:**248–254.
7. **Bustos, S. A., and R. F. Schleif.** 1993. Functional domains of the AraC protein. Proc. Natl. Acad. Sci. USA **90:**5638–5642.
8. **Carra, J. H., and R. F. Schleif.** 1993. Variation of half-site organization and DNA looping by AraC protein. EMBO J. **12:**35–44.
9. **Caswell, R., C. Webster, and S. Busby.** 1992. Studies on the binding of the Escherichia coli MelR transcription activator protein to operator sequences at the MelAB promoter. Biochem. J. **287:**501–508.
10. **Egan, S. M.** 2002. Growing repertoire of AraC/XylS activators. J. Bacteriol. **184:**5529–5532.
11. **Egan, S. M., and R. F. Schleif.** 1993. A regulatory cascade in the induction of *rhaBAD*. J. Mol. Biol. **234:**87–98.
12. **Egan, S. M., and R. F. Schleif.** 1994. DNA-dependent renaturation of an insoluble DNA binding protein. Identification of the RhaS binding site at *rhaBAD*. J. Mol. Biol. **243:**821–829.
13. **Gallegos, M.-T., R. Schleif, A. Bairoch, K. Hofmann, and J. L. Ramos.** 1997. AraC/XylS family of transcriptional regulators. Microbiol. Mol. Biol. Rev. **61:**393–410.
14. **Ghosh, M., and R. F. Schleif.** 2001. Biophysical evidence of arm-domain interactions in AraC. Anal. Biochem. **295:**107–112.
15. **Gottesman, M. E., and M. B. Yarmolinsky.** 1968. The integration and excision of the bacteriophage lambda genome. Cold Spring Harbor Symp. Quant. Biol. **33:**735–747.
16. **Holcroft, C. C., and S. M. Egan.** 2000. Interdependence of activation at *rhaSR* by cyclic AMP receptor protein, the RNA polymerase alpha subunit C-terminal domain, and RhaR. J. Bacteriol. **182:**6774–6782.
17. **Holcroft, C. C., and S. M. Egan.** 2000. Roles of cyclic AMP receptor protein and the carboxyl-terminal domain of the α subunit in transcription activation of the *Escherichia coli rhaBAD* operon. J. Bacteriol. **182:**3529–3535.
18. **Howard, V. J., T. A. Belyaeva, S. J. Busby, and E. I. Hyde.** 2002. DNA binding of the transcription activator protein MelR from Escherichia coli and its C-terminal domain. Nucleic Acids Res. **30:**2692–2700.
19. **Kaldalu, N., U. Toots, V. de Lorenzo, and M. Ustav.** 2000. Functional domains of the TOL plasmid transcription factor XylS. J. Bacteriol. **182:**1118–1126.
20. **Kwon, H. J., M. H. J. Bennik, B. Demple, and T. Ellenberger.** 2000. Crystal structure of the *Escherichia coli* Rob transcription factor in complex with DNA. Nat. Struct. Biol. **7:**424–430.
21. **Martin, R. G., and J. L. Rosner.** 2001. The AraC transcriptional activators. Curr. Opin. Microbiol. **4:**132–137.
22. **Miller, J. H.** 1972. Experiments in molecular genetics. Cold Spring Harbor Laboratory Press, Cold Spring Harbor, NY.
23. **Neidhardt, F. C., P. L. Bloch, and D. F. Smith.** 1974. Culture medium for enterobacteria. J. Bacteriol. **119:**736–747.
24. **Poore, C. A., C. Coker, J. D. Dattelbaum, and H. L. T. Mobley.** 2001. Identification of the domains of UreR, an AraC-like transcriptional regulator of the urease gene cluster in *Proteus mirabilis*. J. Bacteriol. **183:**4526–4535.
25. **Power, J.** 1967. The L-rhamnose genetic system in Escherichia coli K-12. Genetics **55:**557–568.
26. **Prouty, M. G., C. R. Osorio, and K. E. Klose.** 2005. Characterization of functional domains of the Vibrio cholerae virulence regulator ToxT. Mol. Microbiol. **58:**1143–1156.
27. **Reed, W. L., and R. F. Schleif.** 1999. Hemiplegic mutations in AraC protein. J. Mol. Biol. **294:**417–425.
28. **Rhee, S., R. G. Martin, J. L. Rosner, and D. R. Davies.** 1998. A novel DNA-binding motif in MarA: the first structure for an AraC family transcriptional activator. Proc. Natl. Acad. Sci. USA **95:**10413–10418.
29. **Saviola, B., R. Seabold, and R. F. Schleif.** 1998. Arm-domain interactions in AraC. J. Mol. Biol. **278:**539–548.
30. **Schleif, R.** 2000. Regulation of the L-arabinose operon of Escherichia coli. Trends Genet. **16:**559–565.
31. **Seabold, R. R., and R. F. Schleif.** 1998. Apo-AraC actively seeks to loop. J. Mol. Biol. **278:**529–538.
32. **Simons, R. W., F. Houman, and N. Kleckner.** 1987. Improved single and multicopy *lac*-based cloning vectors for protein and operon fusions. Gene **53:**85–96.
33. **Soisson, S. M., B. MacDougall-Shackleton, R. Schleif, and C. Wolberger.** 1997. Structural basis for ligand-regulated oligomerization of AraC. Science **276:**421–425.
34. **Stewart, G. S., S. Lubinsky-Mink, C. G. Jackson, A. Cassel, and J. Kuhn.** 1986. pHG165: a pBR322 copy number derivative of pUC8 for cloning and expression. Plasmid **15:**172–181.
35. **Tate, C. G., J. A. R. Muiry, and P. J. F. Henderson.** 1992. Mapping, cloning, expression, and sequencing of the *rhaT* gene which encodes a novel L-rhamnose-H^+ transport protein in *Salmonella typhimurium* and *Escherichia coli*. J. Biol. Chem. **287:**6923–6932.

36. **Timmes, A., M. Rodgers, and R. Schleif.** 2004. Biochemical and physiological properties of the DNA binding domain of AraC protein. J. Mol. Biol. **340:**731–738.
37. **Tobin, J. F., and R. F. Schleif.** 1987. Positive regulation of the *Escherichia coli* L-rhamnose operon is mediated by the products of tandemly repeated regulatory genes. J. Mol. Biol. **196:**789–799.
38. **Tobin, J. F., and R. F. Schleif.** 1990. Purification and properties of RhaR, the positive regulator of the L-rhamnose operons of *Escherichia coli*. J. Mol. Biol. **211:**75–89.
39. **Tobin, J. F., and R. F. Schleif.** 1990. Transcription from the *rha* operon p_{sr} promoter. J. Mol. Biol. **211:**1–4.
40. **Via, P., J. Badia, L. Baldoma, N. Obradors, and J. Aguilar.** 1996. Transcriptional regulation of the *Escherichia coli rhaT* gene. Microbiology **142:**1833–1840.
41. **Wade, J. T., T. A. Belyaeva, E. I. Hyde, and S. J. Busby.** 2000. Repression of the Escherichia coli *melR* promoter by MelR: evidence that efficient repression requires the formation of a repression loop. Mol. Microbiol. **36:**223–229.
42. **Wickstrum, J. R., and S. M. Egan.** 2004. Amino acid contacts between sigma 70 domain 4 and the transcription activators RhaS and RhaR. J. Bacteriol. **186:**6277–6285.
43. **Wickstrum, J. R., and S. M. Egan.** 2002. Ni+-affinity purification of untagged cyclic AMP receptor protein. BioTechniques **33:**728–730.
44. **Wickstrum, J. R., T. J. Santangelo, and S. M. Egan.** 2005. Cyclic AMP receptor protein and RhaR synergistically activate transcription from the L-rhamnose-responsive *rhaSR* promoter in *Escherichia coli*. J. Bacteriol. **187:**6708–6718.
45. **Wu, M., and R. Schleif.** 2001. Mapping arm-DNA-binding domain interactions in AraC. J. Mol. Biol. **307:**1001–1009.
46. **Wu, M., and R. Schleif.** 2001. Strengthened arm-dimerization domain interactions in AraC. J. Biol. Chem. **276:**2562–2564.
47. **Yanisch-Perron, C., J. Vieira, and J. Messing.** 1985. Improved M13 phage cloning vectors and host strains: nucleotide sequences of the M13mp18 and pUC19 vectors. Gene **33:**103–119.
48. **Zhi, H., and D. J. Jin.** 2003. Purification of highly-active and soluble *Escherichia coli* sigma 70 polypeptide overproduced at low temperature. Methods Enzymol. **370:**174–180.
49. **Zhi, H., W. Yang, and D. J. Jin.** 2003. *Escherichia coli* proteins eluted from mono Q chromatography, a final step during RNA polymerase purification procedure. Methods Enzymol. **370:**291–300.